

## Effect of Anionic 4.5-Generation Polyamidoamine Dendrimer on the Formation of Calcium Carbonate Polymorphs

Kensuke Naka,<sup>\*</sup> Akihiro Kobayashi,<sup>†</sup> and Yoshiki Chujo<sup>\*</sup>

Department of Polymer Chemistry, Graduate School of Engineering, Kyoto University, Kyoto 606-8501

<sup>†</sup>UBE-NITTO KASEI CO., LTD, Gifu 500-8386

(Received May 30, 2002)

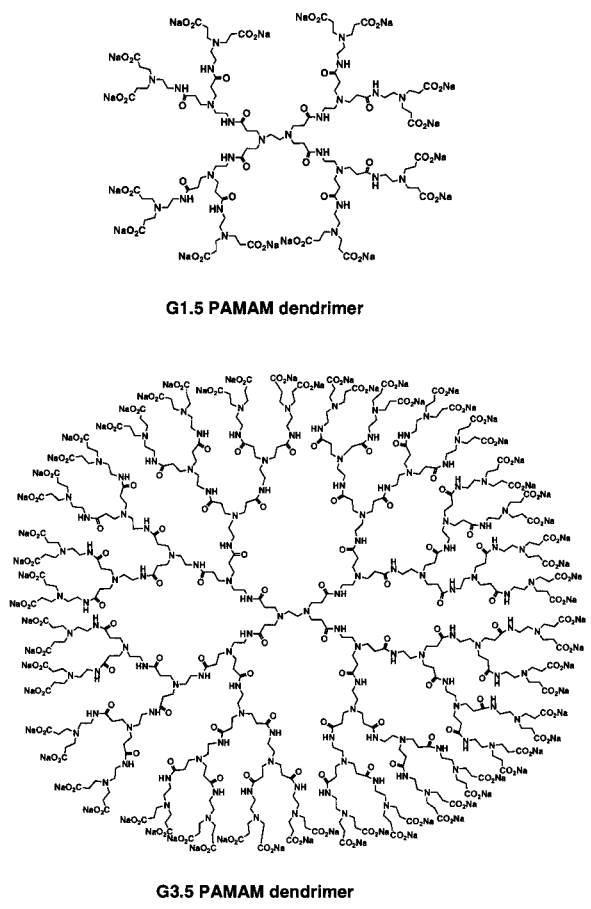
The precipitation of  $\text{CaCO}_3$  in the absence or the presence of the G4.5 PAMAM dendrimer was carried out by a “carbonate diffusion method”. Formation of crystalline  $\text{CaCO}_3$  at different feed ratios of the G4.5 dendrimer to calcium ions was studied with the concentration of calcium ions kept at 0.1 M. Although calcite was predominantly formed at the concentration of the G4.5 PAMAM dendrimer corresponding to 2.65 mM of  $-\text{COONa}$ , the crystal phase of the obtained  $\text{CaCO}_3$  at the higher concentration of the G4.5 PAMAM dendrimer at 5.3 mM consisted entirely of vaterite. As the concentration of  $-\text{COONa}$  increased from 5.3 to 10.6 mM, the particle sizes of the spherical vaterites were reduced from  $8.7 \pm 1.0$  to  $5.2 \pm 3.0 \mu\text{m}$  determined by SEM observation. The crystal phase of the obtained  $\text{CaCO}_3$  in the absence of any additives was a mixture of calcite and vaterite. Although vaterite was predominantly formed by the G4.5 dendrimer, relatively high amounts of calcite were observed in the case of the G3.5 and G1.5 dendrimers. These results suggest that the G4.5 dendrimer more effectively induces vaterite formation compared with the earlier generation of the dendrimers.

The interest of many researchers lies in understanding how organized inorganic materials with complex morphological forms can be produced by biomineralization processes, and how such complexity can be reproducibly synthesized in biomimetic systems.<sup>1,2</sup> In these mineralized tissues, crystal morphology and polymorph, size, and orientation are determined by local conditions and, in particular, by the presence of “matrix” proteins or other macromolecules. Morphological control can be accomplished by adsorption of the soluble additives onto specific faces of growing crystals, altering the relative growth rates of the different crystallographic faces and leading to different crystal habits. These processes usually take place at an organic-inorganic interface, the organic portion providing the initial structural information for the inorganic part to nucleate on and grow outwards in the desired manner. However, there remain many unknowns as to how the matrix affects the crystallization process. Due to the complexity of the natural biomineralization systems, mineralization research has been studied on model organic interfaces. Because the proteins associated with biominerals are usually highly acidic macromolecules, simple polyelectrolytes, such as sodium salts of poly(aspartic acid) and poly(glutamic acid), were examined for the model of biomineralization.<sup>3–5</sup> Studies of inorganic crystallization in the presence of such soluble polymers, models of biogenic proteins, have shown that selectivity for certain crystal faces appears to be highly dependent on the secondary structure of the macromolecules. A recent approach has employed synthetic supramolecular assemblies and structures to offer semi-rigid templates for inorganic crystallization.<sup>6–9</sup>

Calcium carbonate makes up an attractive model mineral for studies in the laboratory, since its crystals are easily characterized and the morphology of  $\text{CaCO}_3$  has been the subject to

control in biomineralization processes. The precipitation of  $\text{CaCO}_3$  in aqueous solution is also of great interest for industrial and technological applications. The particular interest in this system is due to the polymorphism of  $\text{CaCO}_3$ , which has three anhydrous crystalline forms, i.e., vaterite, aragonite, and calcite in order of decreasing solubility and increasing stability. The three polymorphs have markedly different physico-chemical characteristics, and it is often found that less stable forms are stabilized kinetically. Since vaterite transforms easily into thermodynamically most stable calcite via a solvent-mediated process,<sup>10</sup> vaterite is not as wide-spread in nature as the other two polymorphs are. While there can be no doubt that these crystal structures are determined by local conditions in natural systems, the manner in which organisms control polymorph formation and specific biological requirement of the organisms to manipulate both the polymorph and the orientation of the mineral are not well understood.

Poly(amidoamine) (PAMAM) dendrimers with carboxylate groups at the external surface, termed half-generation or  $G = n.5$  dendrimers, have been proposed as mimics of anionic micelles or proteins (Scheme 1).<sup>11,12</sup> The starburst structures are disk-like shapes in the early generations, whereas the surface branch cell becomes substantially more rigid and the structures are spheres in the later generations.<sup>12</sup> Due to unique and well-defined secondary structures of the dendrimers, the anionic dendrimers should be a good candidate for studying the mineralization processes. Recently, we studied the crystallization of  $\text{CaCO}_3$  in the presence of the early generation of the anionic PAMAM dendrimers and found that the anionic dendrimers were habit modifiers and affect crystal morphology of inorganic crystallization.<sup>13,14</sup> A crystallization of  $\text{CaCO}_3$  in the presence of the dendrimers resulted in the formation of spherical



Scheme 1.

vaterite particles whereas rhombohedral calcite crystal was formed without the additives. These preliminary experiments, however, seem to be part of a complex overall story, since crystallization of  $\text{CaCO}_3$  depends on nucleation condition. Here, we studied the effect of the G1.5, G3.5, and G4.5 PAMAM dendrimers by a “carbonate diffusion method” and found that the G4.5 PAMAM dendrimer effectively induced or stabilized a meta-stable crystalline phase of  $\text{CaCO}_3$  in aqueous solution even in the presence of a large excess amount of calcium ions.

### Experimental

**Materials and Methods.** Half-generation poly(amido-amine) (G1.5, G3.5, and G4.5 PAMAM) dendrimers were obtained from Aldrich as sodium salts in methanol. The G1.5, G3.5, and G4.5 PAMAM dendrimers contain 16, 64, and 128 surface carboxylate groups, respectively. Calcium chloride and ammonium carbonate were purchased from WAKO Pure Chemical Industries, Ltd. Scanning electron microscopic (SEM) measurements were carried out with a JEOL JSM-5310/LV at 15KV. The X-ray diffraction and FT-IR were recorded on a Shimadzu XRD-6000 and a Perkin Elmer system 2000, respectively. Vaterite content of  $\text{CaCO}_3$  was determined from the IR measurement on the basis of the absorbances at 877 and  $746\text{ cm}^{-1}$ .

**Crystallization of  $\text{CaCO}_3$ .** A typical precipitation of  $\text{CaCO}_3$  in the presence of the PAMAM dendrimer was carried out as follows. A methanol solution of the G4.5 PAMAM dendrimer (0.55 ml,  $8.3 \times 10^{-2}$  mmol) in a 20 mL plastic cup was dried in vacuum. Then the PAMAM dendrimer was dissolved in 10 mL of

distilled water. Calcium chloride (0.11 g, 1.0 mmol) was added to the aqueous solution of the PAMAM dendrimer. Then the aqueous solution was adjusted to pH 8.5 by aqueous ammonia and was placed in a desiccator with some crushed  $(\text{NH}_4)_2\text{CO}_3$  as a carbonate source. The desiccator was kept at 25 °C for 1 day. A white crystalline product was obtained, collected by filtration, and washed with water, and then dried in vacuum.

**Potentiometric Titrations.** Potentiometric titrations were carried out at 25 °C, with a Horiba D-2 pH meter and a glass electrode. The titrations were performed with 0.01 M HCl in 1.0 M KCl with constant  $-\text{COONa}$  units of the dendrimers. Each methanol solution of the G1.5 ( $1.9 \times 10^{-3}$  mmol), G3.5 ( $4.7 \times 10^{-4}$  mmol), and G4.5 ( $2.3 \times 10^{-4}$  mmol) PAMAM dendrimer corresponding to  $3.0 \times 10^{-2}$  mmol of  $-\text{COONa}$  in a 50 mL vessel was dried in vacuum. Then the PAMAM dendrimer was dissolved in 30 ml of distilled water with KCl (0.22 g,  $3.0 \times 10^{-2}$  mmol). The titration of the dendrimers in the presence of calcium ions was performed by addition of calcium chloride (3.3 mg,  $3.0 \times 10^{-2}$  mmol).

### Results and Discussion

The precipitation of  $\text{CaCO}_3$  in the absence or the presence of the G4.5 PAMAM dendrimer was carried out by a “carbonate diffusion method” similar to the method described by Addadi et al.<sup>15</sup> A solution of the dendrimer with calcium chloride in 200 ml of distilled water was adjusted to pH 8.5 with aqueous  $\text{NH}_3$ . Carbonate was introduced to the solution via vapor diffusion. The critical point of the appearance in the turbidity of the solution was observed at around 5 min. These solutions were kept at 30 °C under  $\text{N}_2$  for 1 day. The crystalline  $\text{CaCO}_3$  was collected and washed with water several times to remove contaminated dendrimers that were not involved in the crystal. Formation of the crystalline  $\text{CaCO}_3$  at different feed ratios of the G4.5 PAMAM dendrimer to calcium ions was studied with the concentration of calcium ions kept at 0.1 M. The results are summarized in Table 1. The dendrimer contents in the crystalline  $\text{CaCO}_3$  of run 2, 3, and 4 determined by elemental analysis were 1.27, 2.40, and 7.27 wt%, respectively. The crystal phase of the obtained  $\text{CaCO}_3$  was characterized by FT-IR analysis.<sup>16</sup> At the low concentration of the G4.5 PAMAM dendrimer (runs 2 and 3), two bands at 877 and  $713\text{ cm}^{-1}$  assigned to the  $v_4$  and  $v_2$  absorption bands of  $\text{CO}_3^{2-}$  in calcite, respectively, were observed (Fig. 1b). This indicates that calcite was predominantly formed. However, as the concentration of  $-\text{COONa}$  increased to 5.3 mM, a band at  $746\text{ cm}^{-1}$  that indicated vaterite formation strongly appeared (Fig. 1c). Further increase of the concentration of  $-\text{COONa}$  to 10.6 mM also formed vaterite. The vaterite content in each sample was determined by IR analysis and value are also summarized in Table 1. The crystal phase of the obtained  $\text{CaCO}_3$  was further confirmed by XRD (Fig. 2). The fraction of vaterite in runs 2 and 4 was 17% and 93% determined by Rao's equation, respectively.<sup>17</sup> These values were in good agreement with those determined by IR. Although calcite was predominantly formed at the concentration of the G4.5 PAMAM dendrimer corresponding to 2.65 mM of  $-\text{COONa}$  (run 3), the crystal phase of the obtained  $\text{CaCO}_3$  at the higher concentration of the G4.5 PAMAM dendrimer at 5.3 mM consisted entirely of vaterite (98% by IR). These results indicate that the presence of

Table 1. The Precipitation of  $\text{CaCO}_3$  in the Absence and the Presence of the G4.5 PAMAM Dendrimer

Run	$[-\text{COONa}] / \text{mM}$	$[\text{Ca}^{2+}] / \text{M}$	$[-\text{COONa}] / [\text{Ca}^{2+}]$	Yield <sup>a)</sup> / %	polymorphs <sup>d)</sup>	Vaterite cont. <sup>b)</sup> / %
1	0	0.1	0	84	Calcite + Vaterite	56
2	0.53	0.1	0.0053	85	Calcite >> Vaterite	15
3	2.65	0.1	0.027	68	Calcite	0
4	5.3	0.1	0.053	91	Vaterite >>> Calcite	98
5	10.6	0.1	0.11	88	Vaterite >>> Calcite	93
6	0	0.05	0	82	Calcite + Vaterite	70
7	0.53	0.05	0.011	75	Calcite	0
8	1.33	0.05	0.027	77	Calcite >>> Vaterite	13
9	2.65	0.05	0.053	82	Vaterite >>> Calcite	89
10	5.3	0.05	0.11	84	Vaterite >>> Calcite	93

a) Based on the total amount of  $\text{Ca}^{2+}$ . b) Polymorphism and the fraction of vaterite were characterized by FTIR.

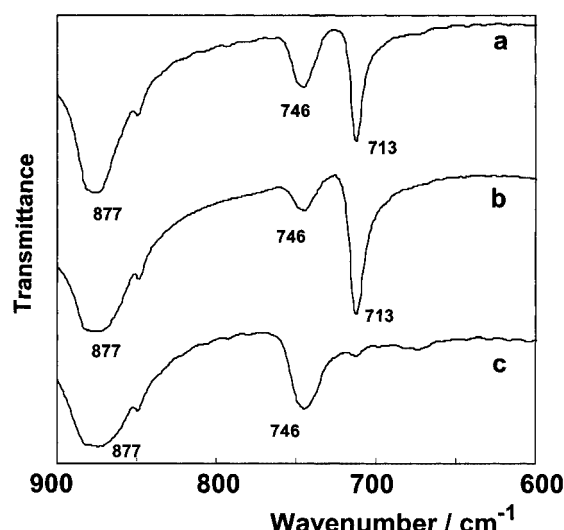


Fig. 1. FT-IR spectra of  $\text{CaCO}_3$  in the absence of the dendrimer (a) and in the presence of (b) 2.65 mM and (c) 5.3 mM of  $-\text{COONa}$  unit of the G4.5 PAMAM dendrimer. Calcium ions were constant at 0.1 M.

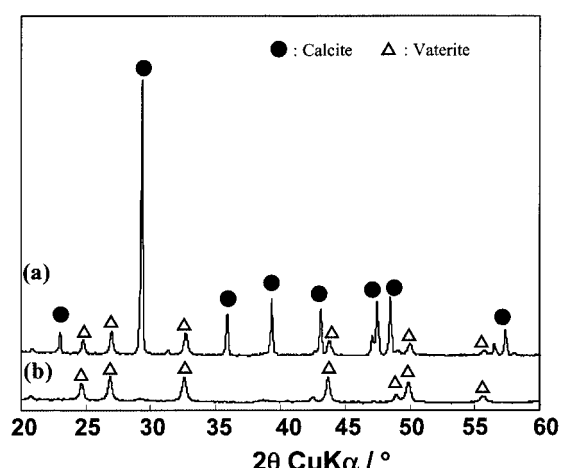


Fig. 2. X-ray diffraction patterns of  $\text{CaCO}_3$  in the presence of (a) 0.53 mM and (b) 5.3 mM of  $-\text{COONa}$  unit of the G4.5 PAMAM dendrimers.

the dendrimer affected polymorphs of  $\text{CaCO}_3$  crystallization.

The precipitation of  $\text{CaCO}_3$  in the absence of any additives was carried out under the same nucleation condition (run 1 in Table 1). The crystal phase of the obtained  $\text{CaCO}_3$  was a mixture of calcite and vaterite as given by IR (Fig. 1a). A band at  $746 \text{ cm}^{-1}$  indicated vaterite formation and bands at  $877$  and  $713 \text{ cm}^{-1}$  were assignable to calcite coexisted. The vaterite content was slightly higher than the calcite content. However, calcite was predominantly formed at the low concentrations of the G4.5 PAMAM dendrimer corresponding to 0.53 and 2.65 mM of  $-\text{COONa}$  (runs 2 and 3). Due to the complexation of the PAMAM dendrimer with calcium ions in aqueous solutions, crystallization of calcium carbonate in the presence of the dendrimer is inhibited compared with that in the absence of the additive with constant concentration of calcium ions.<sup>14</sup> We reported that the saturated concentrations of calcium ions in the presence of the G1.5 and G3.5 PAMAM dendrimers were 1.3 and 2.8 times higher than that in the absence of the additive, respectively. According to the literature, relatively high supersaturations in high pH values favor the precipitation of vaterite.<sup>18</sup> We speculate that the presence of the dendrimer decreased the concentration of free calcium ions which were not bound to the dendrimer, resulting in the higher calcite contents compared with the content in the absence of the dendrimer.

SEM observations showed that the most crystals obtained in the absence and the low concentrations of the G4.5 PAMAM dendrimer were rhombohedral (Figs. 3a and b). In the high concentrations of the G4.5 PAMAM dendrimer, the vaterite products were spherical (Figs. 3c and d). Each shape of  $\text{CaCO}_3$  is a typical morphology for each polymorph. The particle sizes of the spherical vaterite particles obtained in the presence of the PAMAM dendrimer were dependent on the concentration of the dendrimer. As the concentration of  $-\text{COONa}$  increased from 5.3 to 10.6 mM, the particle sizes of the spherical vaterite particles were reduced from  $8.7 \pm 1.0$  to  $5.2 \pm 3.0 \mu\text{m}$ . The spherical vaterite particles are aggregates of vaterite nanocrystals with diameters of 10 to 30 nm.<sup>19</sup> Formation of the vaterite particles involves two processes, i.e. the nucleation of vaterite nanocrystals and the aggregation of the nanocrystals. Aggregation of the nanocrystals in the presence of the higher concentrations of the G4.5 PAMAM dendrimer might be prevented compared to that in the presence of the

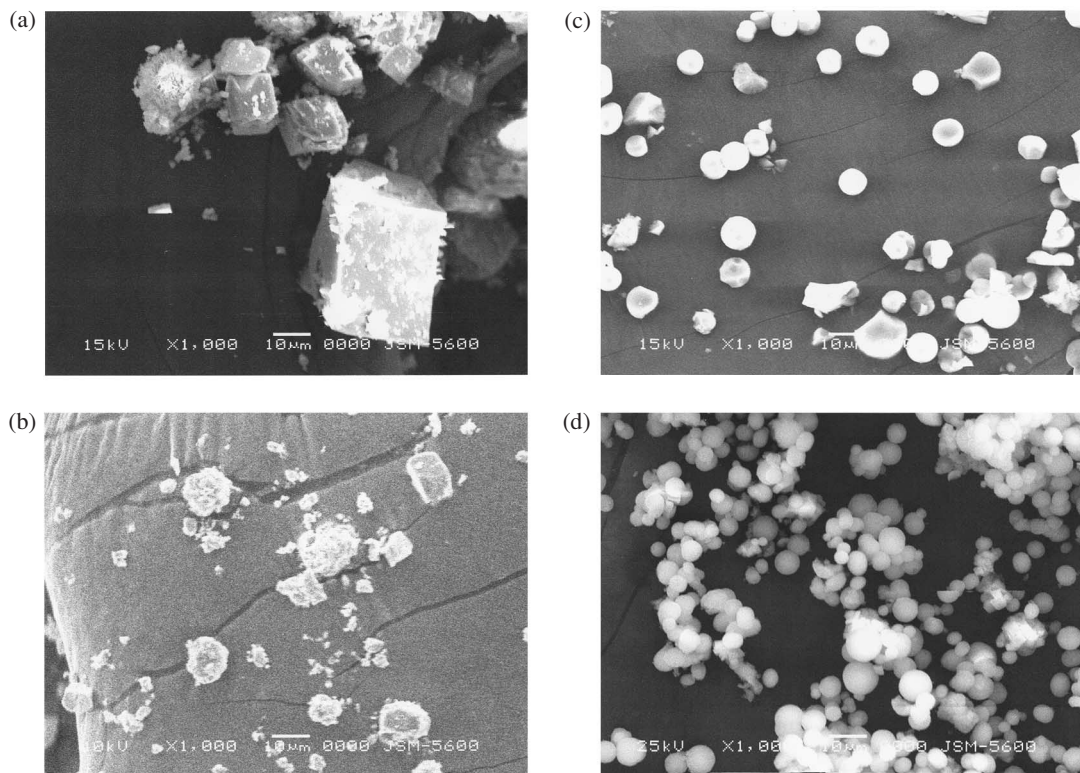


Fig. 3. Scanning electron micrographs of  $\text{CaCO}_3$  in the absence of the dendrimer (a) and in the presence of (b) 2.65 mM, and (c) 5.3 mM and (d) 10.6 mM of -COONa unit of the G4.5 PAMAM dendrimer. Calcium ions were constant at 0.1 M.

lower concentrations of the dendrimer.<sup>14</sup>

The results of the precipitation of  $\text{CaCO}_3$  in the absence and the presence of the G4.5 PAMAM dendrimer at a lower concentration of calcium ion (0.05 M) are also summarized in Table 1. Although the vaterite content was higher than the calcite content in the absence of the dendrimer, calcite was predominantly formed at the concentration of the G4.5 PAMAM dendrimer corresponding to 0.53 and 1.33 mM of -COONa. As the concentration of -COONa increased to 2.65 mM, vaterite formation was strongly induced. At the higher concentration of calcium ions (0.1 M), the critical point of the morphology change from calcite to vaterite was observed on going the concentration of -COONa increased from 2.65 to 5.3 mM. These results indicate that the feed ratio of -COONa and  $\text{Ca}^{2+}$  is a key factor for inducing vaterite formation. In contrast to Figs. 3c and d, SEM observations of the vaterite samples show that ill-defined irregular-shaped and larger-sized aggregates consisting of spherical particles were obtained (Figs. 4a and b). In the general field of colloid chemistry, it is known that fast nucleation relative to growth results in small particle size. The rate of nucleation of vaterite nanocrystal should decrease at the lower concentration of calcium ions. Thus, smaller sized spherical aggregate formation of vaterite nanocrystals might be relatively inhibited compared with that in the higher concentration of calcium ions.

The precipitations of  $\text{CaCO}_3$  in the presence of the G1.5, G3.5, and G4.5 PAMAM dendrimers were carried out with constant -COONa unit and calcium ion concentration of 0.1 M. Although vaterite was predominantly formed by the G4.5 dendrimer, relatively high amounts of calcite was observed in

the case of the G3.5 and G1.5 dendrimers (Table 2). These results suggest that the G4.5 dendrimer more effectively induce vaterite formation compared with the earlier generation of the dendrimers. The calcite content in the G3.5 dendrimer was higher than that in the G1.5 dendrimer. The inner cores of the PAMAM dendrimers are hydrophilic and are potentially open to small hydrophilic molecules, since interior nitrogen moieties would serve as complexation sites.<sup>20,21</sup> At amount of calcium ions on the anionic dendrimers is considerably higher for the later generations than for the early generations. In the same -COONa concentration, the amount of calcium ions entrapped in the PAMAM dendrimers should be higher than that in the later generation of the dendrimer. As shown in the previous report,<sup>14</sup> the saturated concentrations of calcium ions in the presence of the G1.5 and G3.5 PAMAM dendrimers were 1.3 and 2.8 times higher than that in the absence of the additive, respectively. Thus, the later generation dendrimer reduced concentration of free calcium ions which were not bound to the dendrimer, reducing the amount of vaterite.

Later than 4-generation of the PAMAM dendrimers are nearly spherical in shape according to molecular simulations.<sup>22</sup> The half-generation PAMAM dendrimers using various photo-physical probes indicate a structural surface transition in the dendrimer appearance on going from generation 3.5 to 4.5.<sup>20</sup> The morphology of the early generation (0.5–3.5) dendrimers is an open structure, and the internal tertiary amines and amide groups are available for bonding. The later generations have more spheroidal and close-packed surface structures. The protonation behavior of the three generations of the PAMAM dendrimers in 1.0 M KCl is presented in Fig. 5. For the early gen-

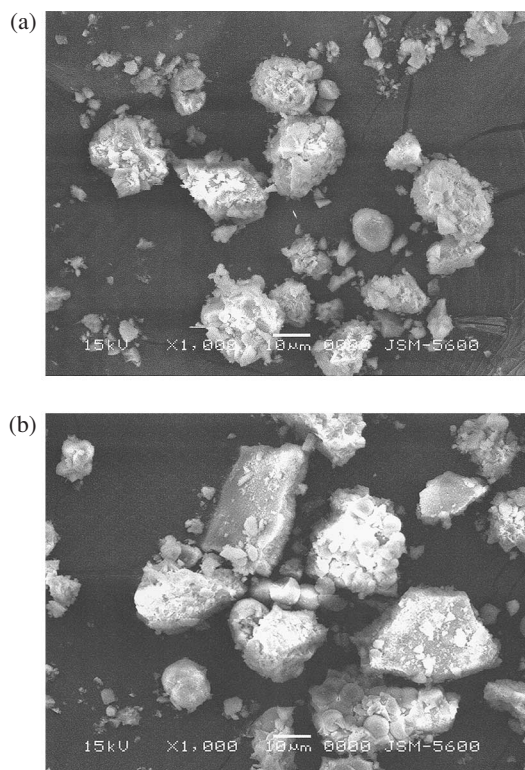


Fig. 4. Scanning electron micrographs of  $\text{CaCO}_3$  in the presence of (a) 2.65 mM, and (b) 5.3 mM of  $-\text{COONa}$  unit of the G4.5 PAMAM dendrimer. Calcium ions were constant at 0.05 M.

eration dendrimers, the rather pronounced difference in dissociation constant between carboxylic groups and amines yields two distinct steps in their titration curves. Only around pH 4 is the carboxylic groups involved in protonation.<sup>23</sup> The titration curves of the G3.5 and G4.5 dendrimers shifted downward in the high pH region, in which the present crystallization took place, compared with that of the G1.5 dendrimer, suggesting that the deprotonation of the ammonium groups of the later generation is easier than that of the early generation by electrostatic repulsions between neighboring amine groups due to their close-packed structures. This indicates that the tertiary amine groups of the later generation can act as more effective bonding sites for cations compared with those of the early generation in the high pH region. Although the amide groups also coordinate with calcium ions, the presence of the internal ammonium groups in the early generation might inhibits the complexation with cations. In the same  $-\text{COONa}$  concentration, the amount of calcium ions entrapped in the PAMAM den-

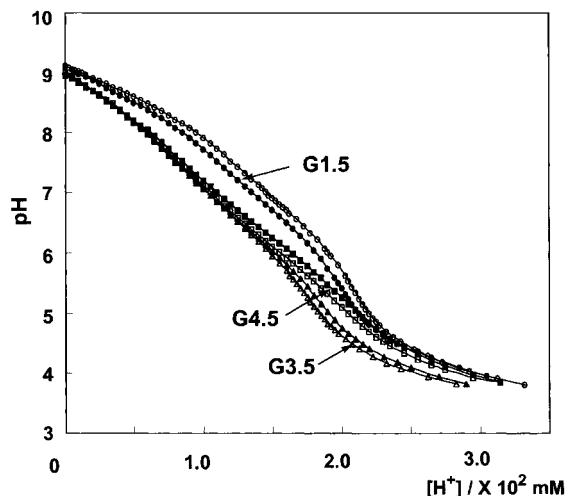


Fig. 5. Potentiometric titrations of the G1.5, G3.5, and G4.5 PAMAM dendrimers in the absence (open symbols) and the presence (close symbols) of calcium ions in 1.0 M KCl solution with 0.01 M HCl solution. The  $-\text{COONa}$  unit of the PAMAM dendrimers was constant at  $3.0 \times 10^{-2}$  mmol.

dimer was higher in the G3.5 dendrimer than that in the G1.5 dendrimer. The titration curve of the G4.5 dendrimer shows no distinct step corresponding to the protonation of the carboxylic groups, suggesting electrostatic repulsions between neighboring carboxylic groups due to the close-packed surface structure.

The titration curves of the dendrimers in the presence of calcium ions are also shown in Fig. 5. In the presence of calcium ions, the titration curve of the G1.5 dendrimer shifted downward, suggesting the chelate formation. The both titration curves of the G3.5 dendrimers in the absence and presence of calcium ions are same especially in the high pH region. The protonation of the G4.5 dendrimer, however, was promoted in the presence of calcium ions. These results indicate that chelation of calcium ions as divalent cations with the coordination sites of the G4.5 dendrimer was inhibited due to reduced flexibility of the structure compared with the early generations. The present mineralization results showed a transition in polymorphous change of  $\text{CaCO}_3$  occurring between G3.5 and G4.5. Although the calcite content increased with increasing the generation from 1.5 to 3.5, the G4.5 dendrimer effectively induced vaterite formation. Complexation properties of the G4.5 dendrimers due to the stereochemical factor would be a major role for the vaterite mineralization.

In the previous reports,<sup>13, 14</sup> the precipitations of  $\text{CaCO}_3$  in the presence of the G1.5, G3.5, and G4.5 PAMAM dendrimers

Table 2. The Precipitation of  $\text{CaCO}_3$  in the Presence of the G1.5, G3.5, and G4.5 PAMAM Dendrimers

Run	Generation	$[-\text{COONa}] / \text{mM}$	$[\text{Ca}^{2+}] / \text{M}$	$[\text{Ca}^{2+}] / [-\text{COONa}]$	Yield <sup>a)</sup> %	Polymorphs <sup>b)</sup>	Vaterite cont. <sup>b)</sup> %
1	1.5	5.3	0.1	0.053	81	Vaterite > Calcite	77
2	3.5	5.3	0.1	0.053	82	Vaterite + Calcite	48
3	4.5	5.3	0.1	0.053	91	Vaterite >> Calcite	98

a) Based on the total amount of  $\text{Ca}^{2+}$ . b) Polymorphism and the fraction of vaterite were characterized by FTIR.

were carried out by a double jet method.<sup>24</sup> In all cases, stable vaterite particles were obtained, in contrast to the present results. Under the previous precipitation condition, extreme supersaturation is achieved at a moment and this provides an immediate nucleation of  $\text{CaCO}_3$ , which is not affected by the organic additives. The nuclei are then immediately transported to regions of lower  $\text{CaCO}_3$  concentration and can grow further. We have shown that spherical vaterite crystals were stabilized by the anionic PAMAM dendrimers in aqueous solution for more than 7 days. Vaterite transforms easily and irreversibly into thermodynamically more stable forms when in contact with water. These results suggested that the surface of the vaterite particles in the previous case was stabilized by the dendrimers to avoid water contact. On the other hand, the vaterite particles obtained in the present case by the carbonate diffusion method were transformed to calcite when the solution was incubated for 4 days. After 4 days incubation in aqueous solution at room temperature, the calcite content in run 4 of Table 1 increased to 87%. Although the dendrimer content in the vaterite particle was 7.27 wt% as determined by elemental analysis, these results indicate that the vaterite surface was not effectively stabilized by the PAMAM dendrimer. Under the present precipitation condition, the dendrimers can play a role in initiating the nucleation of vaterite. Alternatively, the vaterite growth could be explained by a kinetic inhibition of the calcite nuclei by the dendrimers.

### Conclusions

The precipitation of  $\text{CaCO}_3$  in the presence of the anionic PAMAM dendrimers was carried out by the “carbonate diffusion method”, in which a solution of the dendrimers and calcium chloride in distilled water was adjusted to pH 8.5 and carbonate was introduced to the solution via vapor diffusion. Although calcite was predominantly formed at the lower concentration of the G4.5 PAMAM dendrimer, the crystal phase of the obtained  $\text{CaCO}_3$  at the higher concentration of the G4.5 PAMAM dendrimer consisted entirely of vaterite. When the precipitations of  $\text{CaCO}_3$  in the presence of the G1.5, G3.5, and G4.5 PAMAM dendrimers were carried out with constant  $-\text{COONa}$  unit and calcium ions, a transition in polymorphous change of  $\text{CaCO}_3$  occurred between G3.5 and G4.5 as shown in Table 2. The G4.5 PAMAM dendrimer more effectively induce vaterite formation in aqueous solution compared with the early generation dendrimers. This polymorphous transition agreed with a structural surface transition in the half-generations PAMAM dendrimer.<sup>20</sup> Complexation properties of the G4.5 dendrimers would play a major role for the vaterite mineralization. Although the template mechanism of the dendrimers seems to be of a complex nature because simultaneous  $\text{CaCO}_3$  nucleation and interaction with the polymer can be expected, the stereochemical factor is important for the affinity of

the templates to manipulate the polymorph of  $\text{CaCO}_3$ .

We would like to thank Dr. Tetsuo Yazawa and Dr. Koji Kuraoka at Osaka National Research Institute for the XRD analysis.

### References

- 1 K. Naka and Y. Chujo, *Chem. Mater.*, **13**, 3245 (2001).
- 2 L. A. Estroff and A. D. Hamilton, *Chem. Mater.*, **13**, 3227 (2001).
- 3 S. D. Sims, J. M. Didymus, and S. Mann, *J. Chem. Soc., Chem. Commun.*, **1995**, 1031.
- 4 L. A. Gower and D. A. Tirrell, *J. Cryst. Growth*, **191**, 153 (1998).
- 5 Y. Levi, S. Albeck, A. Brack, S. Weiner and L. Addadi, *Chem. Eur. J.*, **4**, 389 (1998).
- 6 J. J. J. M. Donners, B. R. Heywood, E. W. Meijer, R. J. M. Note, C. Roman, A. P. H. J. Schenning, and N. A. J. M. Sommerdijk, *Chem. Commun.*, **2000**, 1937.
- 7 S. Mann, B. R. Heywood, S. Rajam, and J. D. Birchall, *Nature*, **334**, 692 (1988).
- 8 J. Küther and W. Tremel, *Chem. Commun.*, **1997**, 2029.
- 9 J. Lahiri, G. Xu, D. M. Dabbs, N. Yao, I. A. Aksay, and J. T. Groves, *J. Am. Chem. Soc.*, **119**, 5449 (1997).
- 10 D. Kralj, L. Brecevic, and A. E. Nielsen, *J. Cryst. Growth*, **104**, 793 (1990).
- 11 D. A. Tomalia, A. M. Naylor, W. A. Goddard III, *Angew. Chem., Int. Ed. Engl.*, **29**, 138 (1990).
- 12 M.F. Ottaviani, S. Bossmann, N. J. Turro, and D. A. Tomalia, *J. Am. Chem. Soc.*, **116**, 661 (1994).
- 13 K. Naka, Y. Tanaka, Y. Chujo, and Y. Ito, *Chem. Comm.*, **1999**, 1931.
- 14 K. Naka, Y. Tanaka, and Y. Chujo, *Langmuir*, **18**, 3655 (2002).
- 15 L. Addadi, J. Moradian, E. Shay, N. G. Maroudas, and S. Weiner, *Proc. Natl. Acad. Sci., U.S.A.*, **84**, 2732 (1987).
- 16 G. Xu, N. Yao, I. A. Aksay, and J. T. Groves, *J. Am. Chem. Soc.*, **120**, 11977 (1998).
- 17 M. S. Rao, *Bull. Chem. Soc. Jpn.*, **46**, 1414 (1973).
- 18 N. Spanos and P. G. Koutsoukos, *J. Phys. Chem. B*, **102**, 6679 (1998).
- 19 H. Cölfen and M. Antonietti, *Langmuir*, **14**, 582 (1998).
- 20 G. Caminati, N. J. Turro, and D. A. Tomalia, *J. Am. Chem. Soc.*, **112**, 8515 (1990).
- 21 M. C. Moreno-Bondi, G. Orellana, N. J. Turro, and D. A. Tomalia, *Macromolecules*, **23**, 910 (1990).
- 22 A. M. Naylor, W. A. III Goddard, G. E. Kiefer, and D. A. Tomalia, *J. Am. Chem. Soc.*, **111**, 2339 (1989).
- 23 R. C. van Duijvenbode, A. Rajanayagam, G. J. M. Koper, M. W. P. L. Baars, B. F. M. de Waal, E. W. Meijer, and M. Borkovec, *Macromolecules*, **33**, 46 (2000).
- 24 M. Sedláček, M. Antonietti, and H. Cölfen, *Macromol. Chem. Phys.*, **199**, 247 (1998).